Abdominal Radiology

Published online: 18 July 2018

Abdom Radiol (2019) 44:201–208
https://doi.org/10.1007/s00261-018-1694-x

Computed tomography-based texture analysis of bladder cancer: differentiating urothelial carcinoma from micropapillary carcinoma

Ting-wei Fan,[1] Harshawn Malhi,[1] Bino Varghese,[1] Steve Cen,[1] Darryl Hwang,[1] Manju Aron,[1] Nieroshan Rajarubendra,[1] Mihir Desai,[1] and Vinay Duddalwar[1]

[1]Keck School of Medicine of USC, 1975 Zonal Ave, Los Angeles, CA 90033, USA

Abstract

Purpose: The purpose of the study is to determine the feasibility of using computed tomography-based texture analysis (CTTA) in differentiating between urothelial carcinomas (UC) of the bladder from micropapillary carcinomas (MPC) of the bladder.

Methods: Regions of interests (ROIs) of computerized tomography (CT) images of 33 MPCs and 33 UCs were manually segmented and saved. Custom MATLAB code was used to extract voxel information corresponding to the ROI. The segmented tumors were input to a pre-existing radiomics platform with a CTTA panel. A total of 58 texture metrics were extracted using four different texture extraction techniques and statistically analyzed using a Wilcoxon rank-sum test to determine the differences between UCs and MPCs.

Results: Of the 58 texture metrics extracted using the gray level co-occurrence matrix (GLCM) and gray level difference matrix (GLDM), 28 texture metrics were statistically significant ($p < 0.05$) for differences in tumor textures and 27 texture metrics were statistically significant ($p < 0.05$) for peritumoral fat textures. The remaining nine metrics extracted using histogram and fast Fourier transform analyses did not show significant differences between the textures of the tumors and their peritumoral fat.

Conclusions: CTTA shows that MPC have a more heterogeneous texture compared to UC. As visual discrimination of MPC from UC from clinical CT scans are difficult, results from this study suggest that tumor heterogeneity extracted using GLCM and GLDM may be a good imaging aid in segregating MPC from UC. This tool can aid clinicians in further sub-classifying bladder cancers on routine imaging, a process which has potential to alter treatment and patient care.

Key words: Micropapillary carcinoma—Urothelial carcinoma—Texture analysis—Radiomics—Bladder cancer

Bladder cancer is the fourth most common cancer in men, affecting men at four times the rate than affecting women. There will be estimated 62,380 new cases of bladder cancer in men and 18,810 new cases in women for the year 2018 with estimated 17,240 deaths [1]. The majority of bladder cancers are urothelial type cancers in the United States and in Europe, but in Africa where there is a high prevalence of Schistosomiasis, squamous cell carcinoma of the bladder is more common [2, 3].

Micropapillary carcinomas of the bladder (MPCs) are a subset of urothelial carcinomas (UCs) characterized by a histology of tight clusters of micropapillary cells often present in lacunae. Compared to other UC variants, MPCs are known to have a more aggressive clinical course and are associated with a more advanced stage at patient presentation, and consequently, poorer prognoses [4]. Estimates of the incidence of micropapillary carcinoma vary due to its relative rarity, but it is thought to represent up to 8.2% of all UCs [5]. The percentage of the micropapillary component is known to be inversely correlated with prognosis after Bacillus Calmette–Guerin (BCG) therapy, and one study showed that the MPC variant had a five-year survival rate of 73% as compared to similar high-grade UCs of 92.5% [6]. Due to these poor survival rates, some authors advocate more aggressive therapy such as radical cystectomy upon discovery of micropapillary variants to improve survival rates [7]. However, even as of 2014, there is a great degree of variability in the approaches of treating MPCs, as

Correspondence to: Ting-wei Fan; *email:* tingweif@usc.edu

shown by a national survey of urologists and pathologists conducted by Willis et al. [8]. Regardless of the precise treatment strategy, it is clear that earlier detection of MPC subtype would improve patient outcomes compared to later detection.

MPCs are indistinguishable from UCs on direct visualization (i.e., during cystoscopy) and on standard diagnostic CT scans, and pathological examination of a biopsied specimen remains the gold standard for diagnosis [9]. Radiomics, defined as high throughput extraction of imaging features derived from the physical properties of tumors on standard-of-care imaging, and its applications, has been applied to improve diagnostic accuracy as well as potentially impact prognostication from clinical imaging studies. Its use has been demonstrated in a variety of different fields including in the assessments of breast cancers, pleural lesions, gliomas, renal cell carcinomas, and prostate cancers [10–15]. Computed tomography-based texture analysis (CTTA) might be able to improve the diagnostics accuracy of imaging. Specifically, the extraction of features from CT images like tumor texture, using data characterization algorithms developed to extract multiple features using different methods, can allow the conversion of collections of digital radiologic images into mineable data that can be used to quantify bladder tumor behavior and heterogeneity, and aid in identifying the differences in the characteristics of MPCs and UCs.

Studies by Chen et al. and Varghese et al. have shown success in using radiomic analysis to extract quantitative features of renal tumors from clinical standard-of-care CT studies [11, 16, 17]. In this study, we set out to apply the previously used CTTA panel to characterize bladder carcinomas and examine its utility in segregating MPCs from UCs and potentially provide clinicians with a useful diagnostic tool in the management of these patients.

Materials and methods

This study complied with Health Insurance Portability and Accountability Act and was approved by the institutional review board of our institution.

CT data collection, mapping regions of interests (ROIs), and image processing

79 patients with pathologically diagnosed MPC at cystectomy between 1986 and 2015 were identified from a urology database. Patients with CT scans with no digital images or those with incomplete evaluation or with images without contrast enhancement were not included. A fellowship-trained, experienced abdominal radiologist reviewed the imaging of the remaining 33 patients with MPC. The studies were transferred to a dedicated workstation, and Synapse 3D (Fuji Film, Stamford, CT) was used for manual segmentation. Regions of interests (ROIs) were manually drawn for the MPC tumor, perivesicular tissues adjacent to the tumor, normal bladder wall, and normal perivesicular fat. In addition, images of 33 patients with UCs were also analyzed using the same technique for comparison. The DICOM formatted CT images were converted into NIfTI volumes. Custom MATLAB code was used to extract voxel data corresponding to the ROI. 2D CTTA was conducted on the orientation that provided the largest tumor diameter of the tumor ROI. The segmented tumor images were used as inputs to the CTTA panel of a pre-existing radiomics workflow assessing tumor behavior. We evaluated four different types of texture extraction techniques, namely,

(a) histogram analysis (derives first order statistical measures of texture, where only information regarding the gray-level intensity of the pixel is used),
(b) gray-level co-occurrence method (GLCM),
(c) gray-level difference method (GLDM), and
(d) fast Fourier transform methods (FFT).

The latter 3 represent second-order statistical measures of texture, where information regarding the gray-level intensity and their spatial orientation in the image is used. Application of our CTTA panel has been described in previous studies [11, 16, 18], and is summarized in figure (Figs. 1, 2, 3, 4, Table 1).

Statistical method

The purpose of this study is to explore potential novel imaging markers to differentiate MPCs from UCs. We selected the imaging marker based on the difference between MPCs and UCs. When data were normally distributed, such difference was defined by the mean of each imaging marker. When data were not normally distributed, such difference was defined by the mean ranking score of each imaging marker. The data normality was examined by Shapiro–Wilk test and D'Agostino's K^2 test. If both showed normal distribution, the parametric method t test was used. If one of them rejected the normal distribution, the Wilcoxon ranking score transformation was used and followed by a Wilcoxon rank-sum test. Whisker box-plot was used to illustrate the distribution as well as the distance of each imaging marker between MPCs and UCs. To identify robust markers, which were less likely driven by false discovery from multiple comparisons, Bonferroni Step-down (Holm) correction was used. All data analyses were conducted by SAS 9.4.

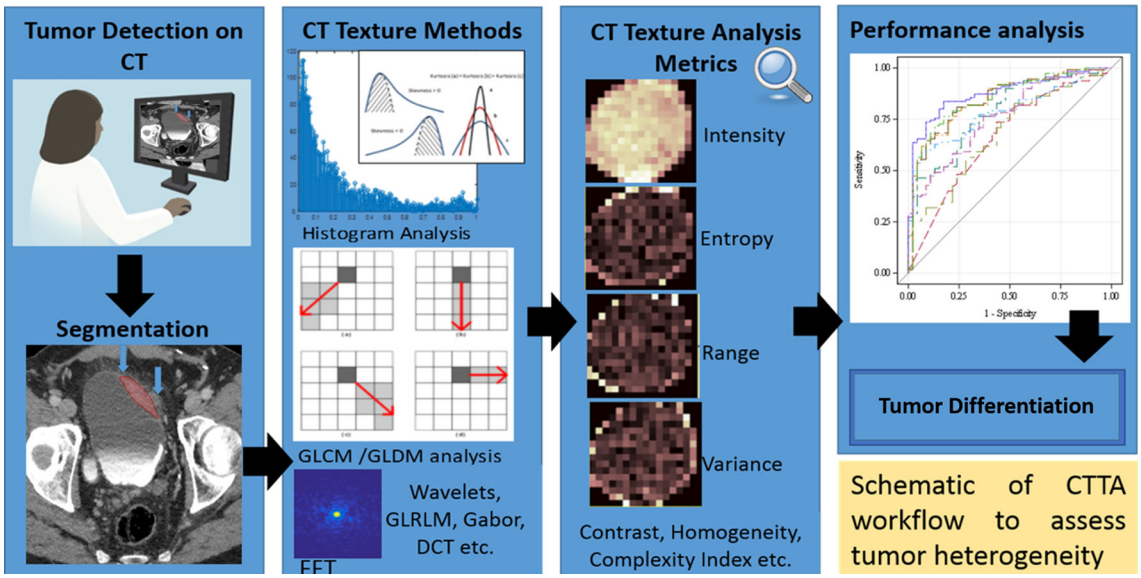

Fig. 1. Workflow of extraction information for CTTA.

Results

33 pathologically verified MPCs and 33 pathologically verified UCs were included in our final study. 14 of 33 UCs were muscle invasive, whereas 31 of 33 MPCs were muscle invasive. Of the 58 texture metrics tested, 28 texture metrics were significant ($p < 0.05$) for differences between UC and MPC tumor characteristics, and 27 texture metrics were significant ($p < 0.05$) for differences between UC and MPC peritumoral fat characteristics.

Tumor texture characteristics demonstrated significant differences ($p \leq 0.01$) in specific GLDM metrics between UCs and MPCs: inverse difference of moment mean (UC: 0.12 ± 0.03, MPC: 0.01 ± 0), sum of average (UC: 8.07 ± 2.1, MPC: 19.41 ± 2.12), difference of average (UC: -21.25 ± 19.39, MPC: -6.7 ± 2.83), information measure of correlation mean (UC: 0.37 ± 0.11, MPC: 0.58 ± 0.12).

Peritumoral fat texture characteristics also demonstrated significant differences in specific GLDM metrics between UCs and MPCs: difference in entropy (UC: 2.52 ± 0.28, MPC: 20.8 ± 0.24), information measure of correlation mean (UC: 0.35 ± 0.09, MPC: 0.67 ± 0.11), inverse difference of moment mean (UC: 0.12 ± 0.03, MPC: 0.01 ± 0.01), and sum of average (UC: 8.39 ± 1.73, MPC: 17.93 ± 2.83).

Discussion

While visual characterization of bladder tumors on clinical imaging may provide suggestions to the diagnosis, it is subject to interobserver variability. In addition, there is often a lack of diagnostic confidence in the visual qualification of imaging data to distinguish the two. Here, we evaluated the utility of CTTA in differentiating MPC from UC. Radiomics is an emerging technique used to extract additional information from diagnostic clinical imaging. From recognizing phenotypes of breast cancer and lung cancers to the differentiation between benign and malignant pancreatic neoplasms, radiomics have been used to distinguish the characteristics of masses not differentiated on visual qualitative evaluation [15, 19, 20]. Using radiomics, defined as high throughput extraction of imaging features derived from the physical properties of the tumors on standard-of-care imaging, we can extract some quantifiable measures to aid in our understanding of disease processes in the human body [18–22].

In this study, we investigated the usefulness of using CTTA to differentiate UC and MPC. We found that there were significant differences between texture characteristics both in the primary tumor as well as the peritumoral/perivesicular fat that correlate the more aggressive MPC with an increase in heterogeneity of the tumor compared with UC. Of interest, a few GLDM texture metrics of the tumor (inverse difference of moment mean, sum of average) were able to use quantitatively and distinctly segregate UCs from MPCs, and some GLDM texture metrics of the peritumoral fat (difference of entropy, information measure of correlation mean) were also able to differentiate UCs from MPCs. We could not identify published literature on texture evaluation of MPC, although one study by Xu et al. developed an algorithm using 13 radiomic features to predict muscle invasiveness of bladder cancer on MRI and another study by Zhang et al. demonstrated feasibility of using CTTA to differentiate low-grade urothelial carcinoma from high-grade urothelial carcinoma [23, 24]. Additionally, Choi et al. proposed the feasibility of using image-based grading of bladder carcinomas, while

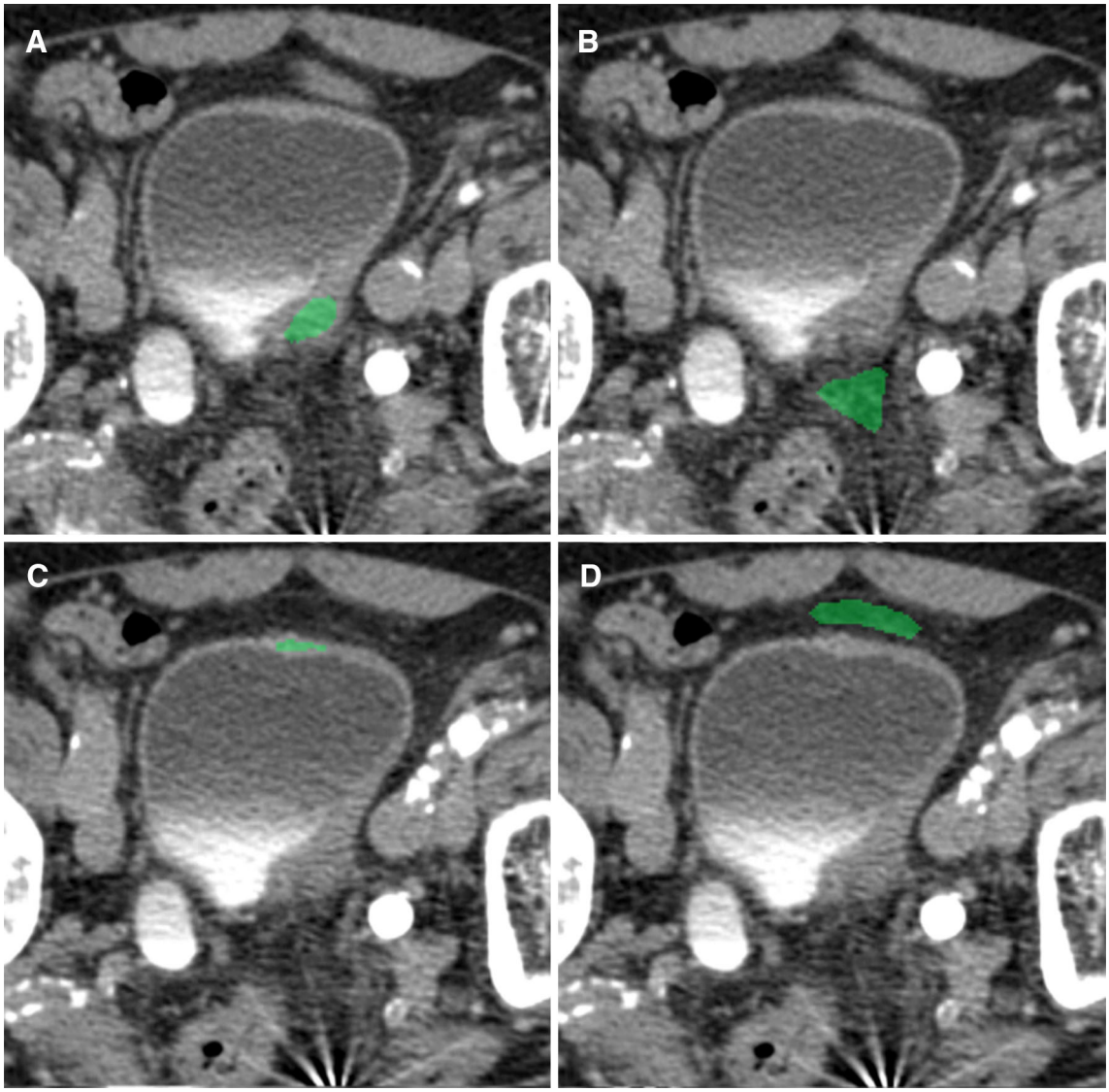

Fig. 2. A 76-year-old male patient with proven MPC variant of muscle-invasive urothelial bladder carcinoma. Regions of interest (in green) were segmented by a fellowship-trained radiologist. **A** MPC variant of urothelial carcinoma in the right posterolateral urinary bladder wall. **B** Peritumoral perivesicular fat in a case of a muscle-invasive MPC. **C** Normal urothelium in the same patient (confirmed on cystoscopy and biopsy). **D** Perivesicular fat adjacent to normal bladder wall.

Mammen et al. associated heterogeneity, both qualitatively and quantitatively, of upper tract urothelial carcinomas with a higher grade and stage of disease [25, 26]. Multiple prior clinical studies report that an increased proportion of micropapillary component of MPC leads to poorer prognosis and a higher risk of being more invasive during the time of presentation [13, 27–29]. Due to the differing types of cells in the MPC and the differing percentages of micropapillary components in MPC, we hypothesize that this biological phenomenon can contribute to the increase in heterogeneity that we found in our study. If this type of heterogeneity can be detected on standard-of-care CT scans, radiomic analyses could provide an objective assessment on the relationship between imaging-based intra-tumoral heterogeneity and physiological phenomena such as tumor grade, biological pathways, and even prognosis. Such pertinent information, from radiologic scans, particularly in scenarios of a high index of suspicion for MPC, could influence the clinician to expedite surgery, or even influence the surgeon to more readily offer early cystectomy or to be more aggressive with resection of the mass by taking a deeper detrusor sampling. As a pilot study, our results demonstrated the feasibility of using radiomics to distinguish between UCs and MPCs, which could result in a decrease in mortality and morbidity of patients with MPCs.

Considering that our quantitative imaging metrics are purely based on the manually segmented inputs of the tumors, these findings, if validated could be translat-

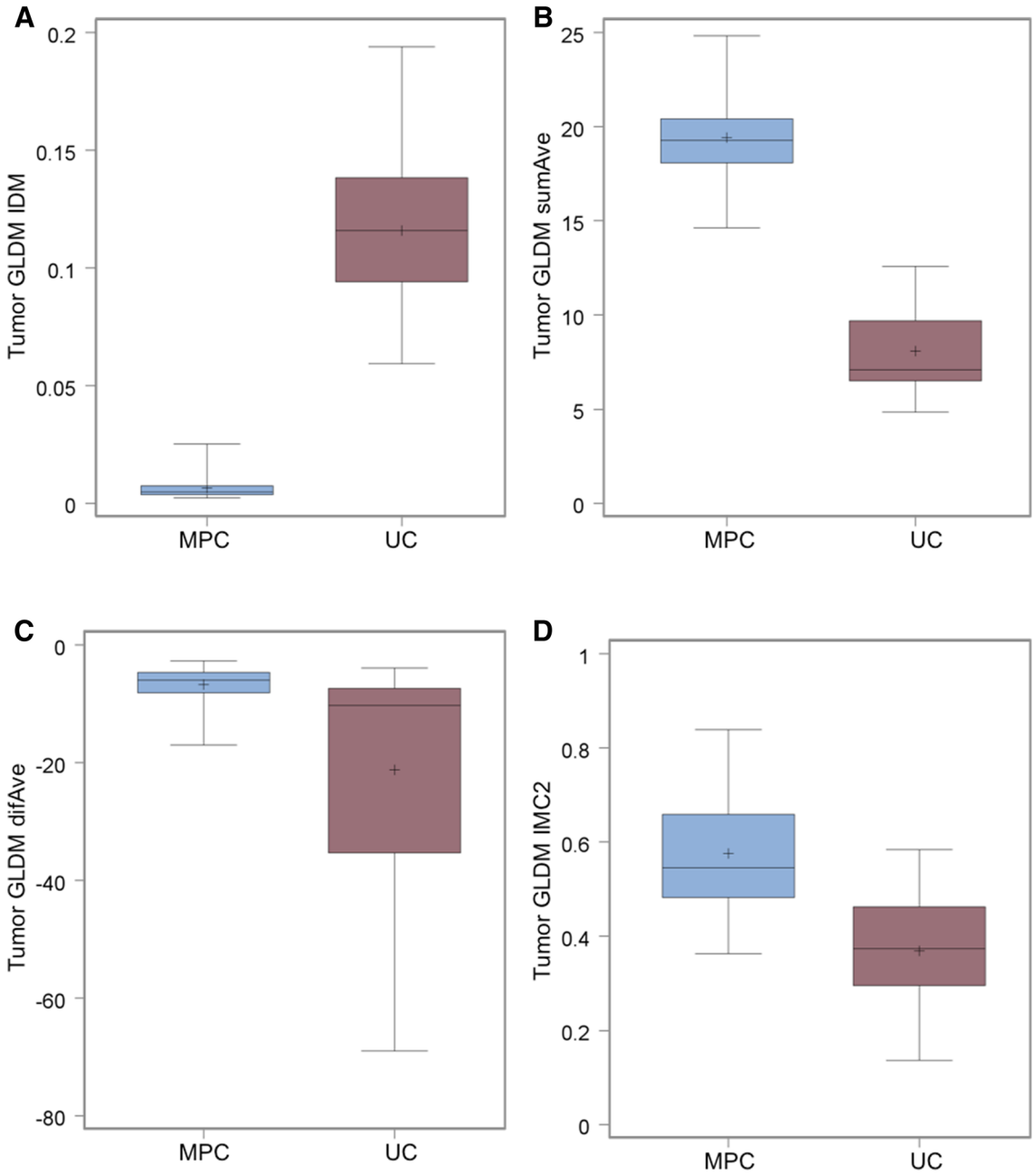

Fig. 3. **A** Whisker box-plot showing the inverse difference moment mean (IDM) of the tumor. MPC (mean: 0.01, standard deviation: 0.00) and UC (mean: 0.12, standard deviation: 0.03) with a p value < 0.01. IDM is a measure of the local homogeneity of an image. IDM feature obtains the measures of closeness of the distribution of the GLDM elements to the GLDM diagonal. **B** Whisker box-plot showing the sum average (sumAve) of the tumor. MPC (mean: 19.41, standard deviation: 2.12) and UC (mean: 8.07, standard deviation: 2.10) with a p value < 0.01. Sum average is a measure of the local heterogeneity of an image. High sumAve values indicate greater heterogeneity. **C** Whisker box-plot showing difference average (diffAve) of the tumor. MPC (mean: $-$ 6.70, standard deviation: 2.83) and UC (mean: $-$ 21.2, standard deviation: 19.39) with a p value < 0.01. Difference average is a measure of the local heterogeneity of an image. High diffAve values indicate greater heterogeneity. **D** Whisker box-plot showing the information measure of correlation 2 mean (IMC2) of the tumor. MPC (mean: 0.58, standard deviation: 0.12) and UC (mean: 0.37, standard deviation: 0.11) with a p value < 0.01. IMC2 is a measure of the local heterogeneity of an image. IMC2 feature obtains the measures of the non-linearity of the grayscale values to its neighbors.

able to other radiologic scans beyond CT, to both 2D and 3D scans and, could be extended to study tumors at other sites in the body. Following large-scale validation, our radiomics framework could provide a solution to

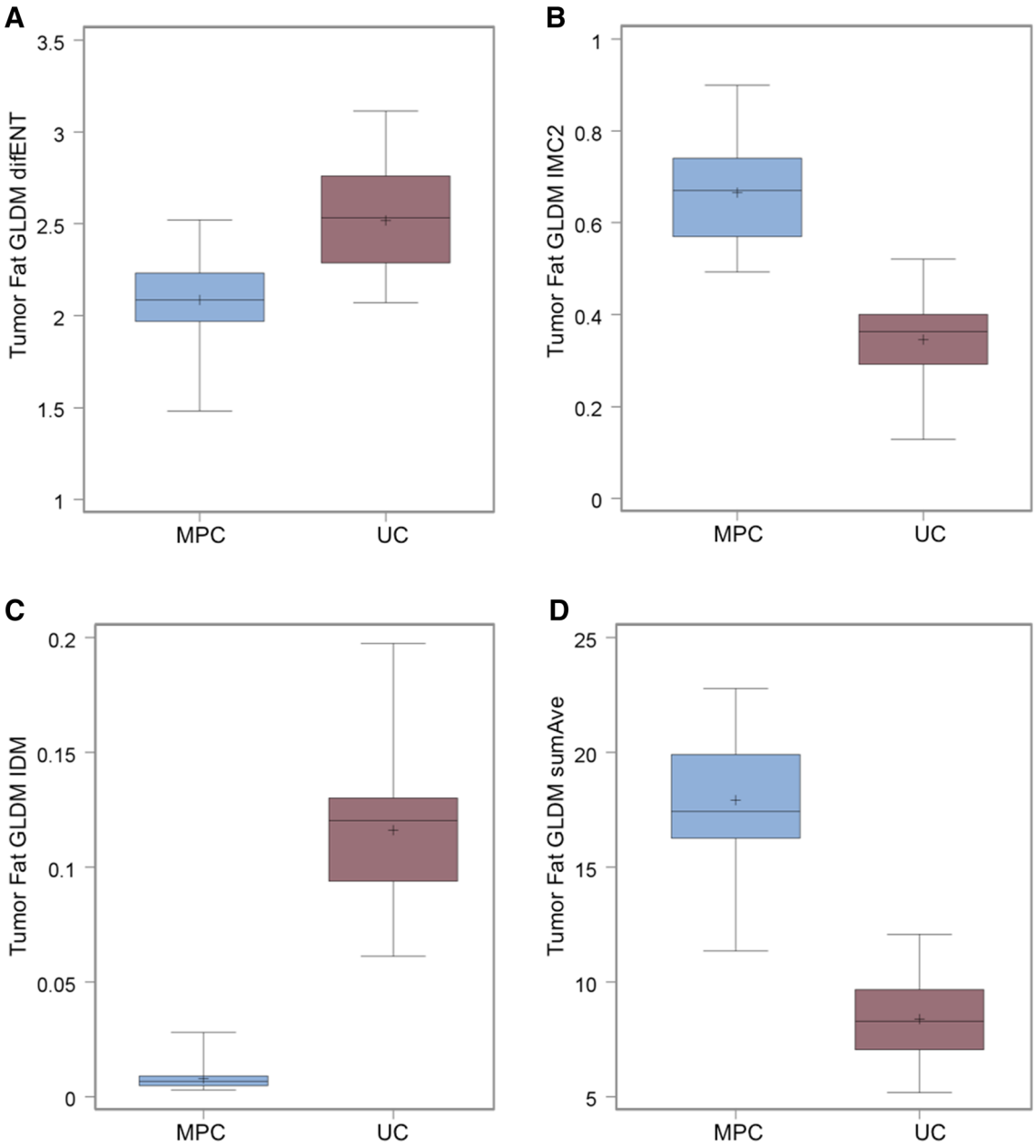

Fig. 4. **a** Whisker box-plot showing the difference in entropy (diffENT) of the peritumoral fat. MPC (mean: 2.08, standard deviation: 0.24) and UC (mean: 2.52, standard deviation: 0.28) with a p value < 0.01. DiffENT is a measure of the local homogeneity of an image. High diffENT values indicate greater homogeneity. **B** Whisker box-plot showing the information measure of correlation 2 mean (IMC2) of the peritumoral fat. MPC (mean: 0.67, standard deviation: 0.11) and UC (mean: 0.35, standard deviation: 0.09) with a p value < 0.01. IMC2 is a measure of the local heterogeneity of an image. IMC2 feature obtains the measures of the non-linearity of the grayscale values to its neighbors. **C** Whisker box-plot showing the inverse difference moment mean (IDM) of the peritumoral fat. MPC (mean: 0.01, standard deviation: 0.01) and UC (mean: 0.12, standard deviation: 0.03) with a p value < 0.01. IDM is a measure of the local homogeneity of an image. IDM feature obtains the measures of the closeness of the distribution of the GLDM elements to the GLDM diagonal. **D** Whisker box-plot showing the sum average (sumAve) of the peritumoral fat. MPC (mean: 17.93, standard deviation: 2.83) and UC (mean: 8.39, standard deviation: 1.73) with a p value < 0.01. Sum average is a measure of the local heterogeneity of an image. High sumAve values indicate greater heterogeneity.

assess intra-tumoral heterogeneity with minimal interruption to the current clinical workflow.

This study had some limitations. First, the small sample size of 33 was limited by the relative rarity of the incidence of MPCs, but our study size is comparable to most studies being conducted recently on MPCs. Chatterjee et al. analyzed clinical, morphological, and immunohistochemical profiles of MPCs with seven pa-

Table 1. Table of metrics measured

Histogram analysis	GLCM/GLDM	Spectral analysis
Kurtosis	Angular second moment	Entropy of FFT mag
Mean	Contrast	Entropy of FFT phase
Quartile range	Correlation	Complexity Index
Standard deviation	Dissimilarity	
Skewness	Entropy	
Median	Homogeneity	
	Inverse difference moment mean	
	Information measures of correlation 1 and 2 mean	
	Measure of correlation coefficient	
	Square root of variance	
	Standard deviation	
	Uniformity	
	Variance	
	Difference average and entropy	
	Sum of average, entropy, and variance	
	Mean	

tients [30]. Many groups have studied the prognosis and differing therapies with 14 MPC patients [6], 17 MPC patients [31], and 33 MPC patients [7]. One of the larger MPC studies studying survival was conducted by Fernandez et al. and Willis et al. with 103 and 283 MPC patients, respectively [32]. Additionally, the study would have benefited from standardization of CT scanners and scanning protocols that were used in studies that were compared. Of our study set of 33 MPCs and TCCs, 31 of 33 MPCs were muscle invasive while only 14 of 33 TCCs were muscle invasive. This is due to the fact that some of the patients had invasive carcinomas diagnosed via transurethral bladder resection, but did not show invasive components after radical cystectomy, and others had received neoadjuvant chemotherapy as well. This could represent a selection bias that could affect the results of our study. In the future, our results would have to be validated with a larger data set.

Conclusion

In conclusion, we found significant differences in texture metrics between UC and MPC, which may indicate increased heterogeneity of MPC compared with UC. As a proof of concept, this illustrates that texture analysis of contrast-enhanced CT images can be developed to quantitatively distinguish between different types of tumors. Further areas of research with larger sample sizes and expansion of radiomic analysis to other types of tumors are needed.

Acknowledgments This research was supported by the Radiological Society of North America Medical Student Grant. We would like to acknowledge Fujifilm and all the personnel at the radiomics laboratory at the University of Southern California for their help with this project.

Compliance with ethical standards

Conflict of interest The authors declare that they have no conflict of interest.

Ethical approval This study has been approved by the appropriate institutional review boards and have been performed in accordance with the ethical standards as laid down in the 1964 Declaration of Helsinki and its later amendments or comparable ethical standards.

Funding RSNA Medical Student Grant (No. RMS172).

References

1. American Cancer Society (2018) *Cancer facts and figures*. Atlanta: American Cancer Society
2. Wong MCS, Fung FDH, Leung C, et al. (2018) The global epidemiology of bladder cancer: a joinpoint regression analysis of its incidence and mortality trends and projection. Sci Rep 8:1129
3. Nielsen ME, Smith AB, Meyer AM, et al. (2013) Trends in stage-specific incidence rates for urothelial carcinoma of the bladder in the United States: 1988 to 2006. Cancer 120:86–95
4. Sui W, Matulay JT, James MB, et al. (2016) Micropapillary bladder cancer: insights from the National Cancer Database. Bladder Cancer 2(4):415–423. https://doi.org/10.3233/blc-160066
5. Kwon GY, Ro JY (2011) Micropapillary variant of urothelial carcinoma. Adv Urol 2011:217153. https://doi.org/10.1155/2011/217153
6. Gofrit ON, Yutkin V, Shapiro A, et al. (2016) The response of variant histology bladder cancer to intravesical immunotherapy compared to conventional cancer. Front Oncol 6:43. https://doi.org/10.3389/fonc.2016.00043
7. Fairey AS, Daneshmand S, Wang L, et al. (2014) Impact of micropapillary urothelial carcinoma variant histology on survival after radical cystectomy. Urol Oncol 32(2):110–116. https://doi.org/10.1016/j.urolonc.2012.04.020
8. Willis DL, Flaig TW, Hansel DE, et al. (2014) Micropapillary bladder cancer: current treatment patterns and review of the literature. Urol Oncol 32(6):826–832
9. Amin MB (2009) Histological variants of urothelial carcinoma: diagnostic, therapeutic and prognostic implications. Mod Pathol 22:S96–S118
10. Zhanx X, Xu X, et al. (2017) Radiomics assessment of bladder cancer grade using texture features from diffusion-weighted imaging. J Magn Reson Imaging. https://doi.org/10.1002/jmri.25669
11. Chen F, Gulati M, Hwang D, et al. (2017) Voxel-based whole-lesion enhancement parameters: a study of its clinical value in differentiating clear cell renal cell carcinoma from renal oncocytoma. Abdom Radiol 42(2):552–560. https://doi.org/10.1007/s00261-016-0891-8
12. Pena E, Ojiaku M, et al. (2017) Can CT and MR shape and textural features differentiate benign versus malignant pleural lesions? Acad Radiol. https://doi.org/10.1016/j.acra.2017.03.006
13. Li Z, Wang Y, et al. (2017) Deep learning based radiomics (DLR) and its usage in noninvasive IDH1 prediction for low grade glioma. Sci Rep 7(1):5467. https://doi.org/10.1038/s41598-017-05848-2

14. Wang J, Wu CJ, et al. (2017) Machine learning-based analysis of MR radiomics can help to improve the diagnostic performance of PI-RADS v2 in clinically relevant prostate cancer. Eur Radiol. https://doi.org/10.1007/s00330-017-4800-5
15. Li H, Zhu Y, Burnside ES, et al. (2016) MR imaging radiomics signatures for predicting the risk of breast cancer recurrence as given by research versions of mammaPrint, oncotype DX, and PAM50 gene assays. Radiology 281(2):382–391. https://doi.org/10.1148/radiol.2016152110
16. Varghese B, Chen F, Hwang D, Cen S, Desai B, Gill I, Duddalwar V. Differentiation of predominantly solid, enhancing lipid-poor renal cell masses using contrast-enhanced computed tomography: evaluating the role of texture in tumor sub-typing. American Journal of Roentgenology (In press)
17. Varghese B, Hwang D, Cen S, et al. (2017) Fast fourier transform based analysis of renal masses on contrast-enhanced computed tomography images for grading of tumor. SPIE Proc. doi 10(1117/12):2256871
18. Huhdanpaa H, Chen F, Hwang D, et al. (2015) CT prediction of the fuhrman grade of clear cell renal cell carcinoma (RCC): towards the development of a quantitative metric. Abdominal Imaging 40(8):3168–3174. https://doi.org/10.1007/s00261-015-0531-8
19. Aerts HJWL, Grossmann P, Tan Y, et al. (2016) Defining a radiomic response phenotype: a pilot study using targeted therapy in NSCLC. Sci Rep 6:33860. https://doi.org/10.1038/srep33860
20. Hanania A, Bantis L, Feng Z, et al. (2016) Quantitative imaging to evaluate malignant potential of IPMNs. Oncotarget 7(52):85776–85784
21. Hodgdon T, McInnes MD, et al. (2015) Can quantitative CT texture analysis be used to differentiate fat-poor renal angiomyolipoma from renal cell carcinoma on unenhanced CT images? Radiology 276(3):787–796
22. Wibmer A, Hricak H, Gondo T, et al. (2015) Haralick texture analysis of prostate MRI: utility for differentiating non-cancerous prostate from prostate cancer and differentiating prostate cancers with different Gleason scores. Eur Radiol 25(10):2840–2850
23. Xu X, Liu Y, Zhang X, et al. (2017) Preoperative prediction of muscular invasiveness of bladder cancer with radiomic features on conventional MRI and its high-order derivative maps. Abdom Radiol (NY) 42(7):1896–1905
24. Zhang GM, Sun H, Shi B, Jin ZY, Xue HD (2017) Quantitative CT texture analysis for evaluating histologic grade of urothelial carcinoma. Abdom Radiol (NY) 42(2):561–568
25. Choi HK, Jarkrans T, Bengtsson E, et al. (1997) Image analysis based grading of bladder carcinoma. Comparison of object, texture and graph based methods and their reproducibility. Anal Cell Pathol 15(1):1–18
26. Mammen S, Krishna S, Quon M, et al. (2018) Diagnostic accuracy of qualitative and quantitative computed tomography analysis for diagnosis of pathological grade and stage in upper tract urothelial cell carcinoma. J Comput Assist Tomogr 42(2):204–210
27. Warrick JI (2017) Clinical significance of histologic variants of bladder cancer. J Natl Compr Cancer Netw 15(10):1268–1274
28. Li Z, Liao H, Tan Z, et al. (2017) Micropaillary bladder cancer: a clinico-pathological characterization and treatment analysis. Clin Transl Oncol 19(10):1217–1224
29. Samaratunga H, Khoo K (2004) Micropapillary variant of urothelial carcinoma of the urinary bladder; a clinicopathological and immunohistochemical study. Histopathology 45:55–64
30. Chatterjee D, Das A, Radotra BD (2015) Invasive micropapillary carcinoma of urinary bladder: a clinicopathological study. Indian J Pathol Microbiol 58(1):2–6. https://doi.org/10.4103/0377-4929.15115
31. Bertz S, Wach S, Taubert H, et al. (2016) Micropapillary morphology is an indicator of poor prognosis in patients with urothelial carcinoma treated with transurethral resection and radiochemotherapy. Virchows Arch 469(3):339–344. https://doi.org/10.1007/s00428-016-1986-x
32. Fernandez MI, Williams SB, Willis DL, et al. (2017) Clinical risk stratification in patients with surgically resectable micropapillary bladder cancer. BJU Int 119(5):684–691. https://doi.org/10.1111/bju.13689